THE EFFECT OF CHANGES IN THE PHYSICAL PARAMETERS OF MICROMETEOROIDS UPON THEIR ABLATION

Joseph J. Kornblum

Space Sciences Division, Ames Research Center, NASA

Moffett Field, California 94035

Running title: Micrometeoroid ablation in the atmosphere

ABSTRACT

The affects of ablation upon stony meteoric particles during their passage through the earths' atmosphere has been examined by Allen, Baldwin, and James [1965] and later by Kornblum [1968 a, b]. In those studies the particles were assumed to be non-rotating spheres of density 3.4 g/cm^3 and the meteoroid vapor pressure law adopted was that proposed for stone by Öpik [1958]. The effects of changes in the physical parameters of the meteoroid, such as the density and the vapor pressure law, upon the ablation is the subject of this investigation. The analysis made use of the above Allen, Baldwin, and James [1965] ablation model together with the assumption that the front and rear face temperatures of the meteoritoid are the same. This assumption allowed the use of a general similarity variable, $\delta r_\infty \cos Z_\infty$ where δ is the meteoroid density, r_∞ the entry radius, and Z_∞ the zenith entry angle. Similarity means that all particles which have the same $\delta r_\infty \cos Z_\infty$ value have the same $\bar{r}$, velocity, and temperature histories, where $\bar{r}$ is defined as the ratio of the instantaneous radius to the entry radius. The use of a similarity variable allows a great simplicity in the analysis and a tremendous saving in computation time. Various proposed meteoroid vapor pressure laws were examined and it was determined that the Norton County Achondrite and the Öpik Iron vapor pressure laws would give the minimum ablation and that the Öpik stone and a synthetic carbonaceous chondrite vapor pressure law would give the maximum ablation. For these four vapor pressure laws the size, velocity, temperature, and shielding histories of meteoroids were calculated for entry velocities of 12, 15, 20, 30, 40,

50, 60, and 70 km/sec. The general similarity variable $\delta r_\infty \cos Z_\infty$ was varied from 0.25 kg/m^3 to 5×10^{-6} kg/m^3. Results are presented as a function of the general similarity variable $\delta r_\infty \cos Z_\infty$ and include for each of the vapor pressure laws the ratio of the residual radius to the entry radius, the maximum temperature reached, and the altitude where ablation ceases. Also presented are graphs of the residual radius vs the entry radius for particular values of $\delta \cos Z_\infty$. The analysis is applicable to particles for which the general similarity variable $\delta r_\infty \cos Z_\infty$, is less than about 0.25 kg/m^3. Over the range of the general similarity variable examined it is found that ablation is important in changing the size distribution of micrometeoroids, especially for particles with entry velocities of 30 km/sec. and greater.

The Effect of Changes in the Physical Parameters of Micrometeoroid Upon Their Ablation

Joseph J. Kornblum

In order to determine the mass and particle flux entering the earth's atmosphere as a function of the size of the particles from rocket, balloon, or ground based collections, the size changes of the particles due to ablation in the atmosphere must be determined. Prior studies to determine flux from sounding rocket collections have assumed that no mass loss by ablation occurs when the radius of the entering particle is less than 50 microns.

Allen, Baldwin, and James [1965] in a recent study have examined the effect of ablation upon meteoric particles. Allen et. al. calculated the radius change due to ablation of assumed spherical non-rotating particles as they decelerated from entry velocity to 0.5 km/sec. They considered several types of material including stone over a range of the similarity variable, entry radius x cos (entry angle), $r_\infty \cos Z_\infty$, from 0.05 to 5,000 microns. Kornblum [1968 a] used the Allen, Baldwin, and James ablation model in calculating the size and velocity history of stony micrometeoroids from entry velocity through kinetic terminal velocity. A density for stone of 3.4 g/cm^3 was assumed. The values of the constants c_1 and c_2 adopted in the meteoroid vapor pressure law

$$\text{Log } p = c_1 + c_2/T \tag{1}$$

were those suggested for stone by Öpik [1958], c_1 equal to 9.6 and c_2 equal to -1.35×10^4. Using the particle histories determined above Kornblum [1968 b] calculated the concentration of micro meteorites in the atmosphere and presented a method of predicting particle collections by sounding rocket and balloon collecting techniques.

The results of Allen, Baldwin, and James [1965] and Kornblum , [1968 a, b] indicate that ablation significantly changes the size distribution. of micron sized particles. The question arises as to how sensitive are these results to the value of the meteorite density and vapor pressure law adopted. It is the purpose of this paper to examine this question.

Analysis

Allen, Baldwin, and James Ablation Model: This model forms the starting point of this investigation and is summarized below. The reader is referred to the paper [Allen et. al. 1965] for derivations of equations. The assumptions underling this ablation model have been discussed by Allen et. al. [1965] and Kornblum [1968 a].

The equation of particle motion is

$$\frac{dv}{dh} = -\frac{g}{v} + \frac{3\gamma v \rho}{4\delta r_\infty \cos Z_\infty \bar{r}} \tag{2}$$

where r_∞ is radius at entry, r the radius of the meteoroid at any time t corresponding to altitude h, and $\bar{r}$ the dimensionless radius r/r_∞. The drag coefficient is γ, and δ is the particle density. Z is the entry angle measured from the vertical, g is the acceleration of gravity, and v is the instantaneous velocity at altitude h.

A temperature difference may exist between the front and rear faces of the meteoroid. To estimate this effect, the body is treated as a cylindrical slab of thickness equal to the radius. The heat conduction equation becomes, therefore,

$$\frac{k}{r_\infty \bar{r}} (T_1 - T_2) = \epsilon\sigma T_2^4 + \zeta w_2 \tag{3}$$

where k is the thermal conductivity of the meteoroid, ϵ the radiation emissivity, ζ the energy required to vaporize a unit mass of the meteorites and w_2 the mass evaporation rate. T_1 and T_2 refer to the front and rear face temperatures respectively.

The size change due to ablation is given by

$$\frac{d\bar{r}}{dh} = \frac{w_1 + w_2}{2v\delta r_\infty \cos Z_\infty} \tag{4}$$

The mass evaporation rate from the front and rear face is, respectively,

$$w_1 = \frac{bp_1}{\sqrt{2\pi R T_1}} = \frac{b \times 10^{c_1 + c_2/T_1}}{\sqrt{2\pi R T_1}} \tag{5}$$

$$w_2 = \frac{bp_2}{\sqrt{2\pi R T_2}} = \frac{b \times 10^{c_1 + c_2/T_2}}{\sqrt{2\pi R T_2}} \tag{6}$$

because the vapor pressure law is of the form

$$\log p = c_1 + (c_2/T) \tag{7}$$

where b is the sticking coefficient and R is the gas constant and is given by $8.3143/\mu$ where μ is the molecular weight of the meteoroid vapors.

The energy input to the meteoroid is assumed to be expended by radiation and ablation processes only. The energy balance equation per unit area per unit time is, therefore,

$$\frac{1}{4} \lambda \rho v^3 = \epsilon\sigma(T_1^{\,4} + T_2^{\,4}) + \zeta(w_1 + w_2). \tag{8}$$

Complete accommodation of the air molecules is assumed. Thus

$$\lambda = 1 \tag{9}$$

With complete accommodation, the drag coefficient would be unity. However, a vaporization correction to the drag force may exist due to a difference in the front and rear face evaporization rates. This correction is given by

$$\gamma_v = \frac{1}{2} \frac{p_1 - p_2}{\rho v^2} \tag{10}$$

The total drag coefficient is then

$$\gamma = 1 + \gamma_v \tag{11}$$

The shielding due to the meteoroid vapors is estimated by calculating the total cross section, Ψ, of all vapor molecules in a stream tube of unit area in front of the body and is given by

$$\Psi = \frac{6.02 \times 10^{23} \pi d^2 \ r_\infty}{\mu R} \left[\frac{\bar{r} \ 10^{c_1 + c_2/T_1}}{T_1} \right] \tag{12}$$

where d is the average diameter and μ the molecular weight of the meteoroid vapor molecules.

Several types of materials including stone were considered over a range of $r_\infty \cos Z_\infty$ from 0.05 to 5000 microns by Allen et. al. [1965]. Allen et. al. terminated their calculations when the velocity became less than 500 m/sec.

The quantity $r_\infty \cos Z_\infty$ behaves as a similarity variable except in the heat conduction equation (3). Similarity means, for example, that a 25 micron radius particle entering vertically, $\cos Z = 1.0$, with a velocity v_1, and a 50 micron radius particle entering at 60° to the vertical, $\cos Z = 0.5$, with the same entering velocity, will have the same $\bar{r}$ and velocity change with altitude. Allen, Baldwin, and James have shown that the error introduced by (3) in treating $r_\infty \cos Z_\infty$ as a proper similarity variable is not significant.

The Allen, Baldwin, and James model applies to free molecular conditions. Kornblum [1968 a] later showed how the model may be extended to follow the particle to kinetic terminal velocity while still maintaining the use of the similarity variable.

General Similarity Variable: The results of Allen et al. [1965] and of Kornblum [1968 a] indicate that the front and rear face temperatures do not differ significantly when $r_\infty \cos Z_\infty$ is less than about 50×10^{-6} meters. For vertical incidence this would refer to particles of about 50 micron radius and less.

Assuming that the front and rear face temperatures are equal,

$$T_2 = T_1 \tag{13}$$

then equations (3) and (10) drop out and there remains only the following equations

$$\frac{dv}{dh} = -\frac{g}{v} + \frac{3\rho v \gamma}{4\bar{r}(\delta r_\infty \cos Z_\infty)} \tag{14}$$

$$\frac{d\bar{r}}{dh} = \frac{b\ 10^{c_1 + c_2/T}}{(2\pi RT)^{1/2}\ v(\delta r_\infty \cos Z_\infty)} \tag{15}$$

$$\frac{\lambda\rho v^3}{8} = \varepsilon\sigma T^4 + \frac{b\zeta\ 10^{c_1+c_2/T}}{(2\pi RT)^{1/2}} \tag{16}$$

These equations allow the use of a more general similarity variable, the density x entry radius x cos (entry angle), $\delta r_\infty \cos Z_\infty$. Equations (14) - (16) together with the use of the similarity variable, $\delta r_\infty \cos Z_\infty$, enable the effects of changing the meteoroid vapor pressure law constants, c_1 and

c_2, and the meteoroid density δ, to be simply evaluated for particles whose rear face temperature is the same as the front face temperature. This means restricting $r_\infty \cos Z_\infty$ to values less than around 50 microns. The use of the above model when T_2 is less than T_1 would result in over estimating the ablation.

Multiplying Ψ by $\delta \cos Z_\infty$ gives

$$S \equiv \Psi \delta \cos Z_\infty = \frac{6.02 \times 10^{23} \pi d^2 (\delta r_\infty \cos Z_\infty)}{\mu R} \left[\frac{r\; 10^{\overline{c_1 + c_2/T}}}{T} \right] \tag{18}$$

The use of the parameter S enables the shielding to be evaluated using the general ablation variable $\delta r_\infty \cos Z_\infty$.

The values of constants adopted are

$\epsilon = 0.92$

$\sigma = 5.6697 \times 10^{-8}\ \mathrm{W/m^2 \text{-} {}^\circ K^4}$

$b = 1.0$

$\mu = 0.05$ kg/mole

$\frac{1}{\sqrt{2\pi R}} = 0.0309$

$d = 2 \times 10^{-10}$ m

The accomodation coefficient λ and the drag coefficient γ are both unity.

Various proposed meteoric vapor pressure laws are given in Table 1. The energy E_R dissipated by radiation processes per unit area per second and E_v the energy dissipated by vaporization processes per unit area per second by the meteorite for several vapor pressure laws is shown in Figure 1. The sum of E_R and E_v when it differs significantly from E_R or E_v is shown by dashed lines. E_R and E_v represent the first and second terms of the right hand side of equation (16) which describes the way in which the energy received is dissipated. Only the volatile part of the carbonaceous chondrite vapor pressure law is shown. The Liebedinec stone vapor pressure law is not shown as it is almost identical to the Norton County Achondrite vapor pressure law.

It is seen from Figure 1 that for a given aborbed energy the Öpik stone and the carbonaceous chondrite vapor pressure laws give the most vaporization. The Öpik Iron and the Norton County Achondrite vapor pressure laws give the least ablation. Computations were carried out for these four vapor pressure laws in order to evaluate the maximum and minimum ablation that could be predicted for micron sized meteoroids. The cases for which computations were made are shown in Table 2. For each value of the entry velocity, computations were made for values of the similarity variable $\delta r_\infty \cos Z_\infty$ starting from 250×10^{-3} kg/m^2 and decreasing to 0.005×10^3 kg/m^2. Whenever a value of $\delta r_\infty \cos Z_\infty$ was reached for which $\bar{r}$ remained 1, implying no ablation takes place, smaller values of $\delta r_\infty \cos Z_\infty$ were not examined for that entry velocity.

For each case, $\bar{r}$, v, T, and S were calculated as a function of the altitude and the results stored on tape for future reference. Computations were made on the Ames Research Center IBM 7094 computer. A starting altitude of 200 km. was adopted. Previous results of Kornblum [1968 a] showed that effective interaction with the atmosphere did not occur until altitudes below 135 km. Computations ceased whenever $\bar{r}$ become less than 10^{-3}, or the velocity became less than the kinetic terminal velocity V_k, or the altitude became less than 55 km. The kinetic terminal velocity, V_k, is given by

$$V_k = \frac{0.733\, g\, \bar{r}\, (\delta r_\infty \cos Z_\infty)}{\rho\, \bar{c}} \qquad (20)$$

where $\bar{c}$ is the mean molecular air velocity. Atmospheric parameters were taken from the 1962 U. S. Standard Atmosphere.

Results and Discussion

The ratio of the final radius to the initial radius (the final value of $\bar{r}$) is shown in Figures 2-5 as a function of the similarity variable, $\delta r_\infty \cos Z_\infty$

for the various vapor pressure laws. Thus, for example, one determined from Figure 5 for the Öpik stone vapor pressure law, that for a value of $\delta r_\infty \cos Z_\infty$ of 10^{-2}kg/m^2 the ratio of the final radius to the initial radius is 0.2 for an entry velocity of 30 km/sec. Thus for an assumed density of stone of 3.4×10^3kg/m^3 (=3.4 g/cm^3) a 6 micron radius particle entering at 60° to the vertical ($\cos Z = 0.5$) would be ablated to a 1.2 micron radius particle.

For random impact upon a gravitating sphere the probability distribution of entry angles [Shoemaker, 1965] is given by

$$p\,Z = \sin 2Z\, d\,Z \qquad (21)$$

The most probable angle of entry is 45°. Equation (21) implies that 1% of the particles impacting have entry angles greater than 85° and 7% have entry angles greater than 75°. In the Allen, Baldwin, and James ablation model, the smallest value of cos Z for which the similarity variable $r_\infty \cos Z_\infty$ is still a valid approximation is about 0.25 corresponding to an angle 75°. Thus the present ablation model should be valid for at least 93% of the entering particles.

In Figures 6-9 the residual radius is plotted against the entry radius for the various vapor pressure laws for a value of $\delta \cos Z_\infty$ of 3.4×10^3 kg/m^3. This would refer to stones of density 3.4 g/cm^3 entering vertically or to higher values of the density at different entry angles. Figures 10-13 show the results for a value of $\delta \cos Z_\infty$ of 0.85×10^3 kg/m^3. This would refer, for example, to particles of density 3.4 g/cm^3 entering at 75° to the vertical, or to particles of density 1 g/cm^3 entering at 31° to the vertical, or to particles of density 0.85 g/cm^3 entering vertically.

Examining Figures 2-13 indicates that the Öpik stone vapor pressure law gives the most ablation while the Norton county Achondrite vapor pressure law gives the least ablation. However, even for the Norton County Achondrite vapor pressure laws ablation is significant for particles of 10 micron radius and larger at entry velocities of 30 km/sec and greater. Decreasing the density results in decreasing the ablation.

In Table 3 the residual radius for a 30μ radius particle entering vertically at 30 km/sec is shown for various assumed meteorite densities and possible vapor pressure laws. It is seen that for a given density the variation in the residual radius as the vapor pressure law is varied from the Norton County Achondrite law to the Öpik stone law is between factors of 5 to 6 on the average. For a given vapor pressure law, halving the value of the meteorite density results, on the average, in a factor of between 3 to 4 times increase in the residual radius.

From Figures 6-13 it is seen that the restriction of size imposed by requiring T_2 equal to T_1 is important only for particles with entry velocities less than 20 km/sec. For higher entry velocities, the larger size particles for which a front and rear face temperature difference would exist are completely ablated and this result should be unchanged by consideration of such a temperature difference.

In Figure 14 the altitude where ablation ceases is shown for the various vapor pressure laws. Only cases for which the ratio of the final value of the radius to the initial radius was less than 0.98 were plotted. The altitude range is from 75 to 120 km.

The maximum temperature reached is shown as a function of the similarity variable $\delta\, r_\infty \cos Z_\infty$ in Figure 15 for the various vapor pressure laws. It is interesting to note that while the Norton County Achondrite vapor pressure law gives the least ablation, it gives the highest temperatures compared to the other vapor pressure laws.

In Table 4 the shielding Ψ ($=S/\delta \cos Z_\infty$) is shown for the Öpik stone and the Norton County Achondrite vapor pressure laws for a value of $\delta \cos Z_\infty$ equal to 10^3kg/m^3. This corresponds to particles of density 1 g/cm^3 entering vertically. For larger values of $\delta \cos Z_\infty$ the shielding is proportionately reduced. The shielding is shown only for the four largest radii examined. The value of these radii are determined by dividing the similarity variable $\delta\, r_\infty \cos Z_\infty$ by the value assigned to $\delta \cos Z_\infty$. Thus when calculating the shielding for a different density, both the value of the shielding and the corresponding particle size will be changed.

When the shielding is evaluated for stones of density 3.4 g/cm^3 ($\delta \cos Z = 3.4 \times 10^3\ \text{kg/m}^3$) and compared to the values calculated by Allen et. al. [1965] , their values are found to be between one and a half to two times larger than the values calculated in this paper. This is within reasonable agreement as the shielding is a very sensitive function of the temperature. Also, Allen et. al. [1965] used the 1959 ARDC model atmosphere while the present work used the 1962 U. S. Standard Atmosphere.

When Ψ equals one there is complete shielding; that is, every incoming atmospheric molecules should undergo at least one collision with a meteoroid vapor molecule. The efficiency of such collisions in reducing the total energy transferred to the meteoroid is very difficult to evaluate, but it seems probable that not too much energy should be lost until the incoming air molecules undergo multiple collisions. Hence a reasonable upper limit for the neglect of shielding might be Ψ equal to 0.5. Even when Ψ equals 1.0 the effects might not be overly important. For assumed meteoroid densities greater than 1 g/cm^3, the shielding can be neglected for values of the similarity variable less than about $200 \times 10^{-3}\ \text{kg/m}^3$.

Concluding Remarks: A method of calculating the particle histories of micrometeoroids in their passage thru the atmosphere has been presented which makes use of a new similarity variable: meteoroid density x entry radius x cos (zenith entry angle). The use of such a similarity variable allows a great simplicity in the analysis and a tremendous saving in computation time.

The effects of changes in the physical parameters of the meteoroid, such as the density and the vapor pressure law, were evaluated. For a given vapor pressure law, halving the value of the meteoroid density increases the residual radius on the average by a factor of 3 to 4. The Norton County Achondrite vapor pressure law gives the minimum ablation, and the Öpik stone vapor pressure law gives the maximum ablation. For a given meteoroid density the residual radius from the Norton County Achondrite vapor pressure law is on the average a factor of 5 to 6 times larger than the residual radius for the Öpik stone vapor pressure law.

For all the meteoroid vapor pressure laws examined, ablation was found to be important in changing the size distribution of micrometeoroids, especially for particles with entry velocities of 30 km/sec and greater.

REFERENCES

Allen, H., B. Baldwin Jr., and N. James, Effect on meteor flight of cooling by radiation and ablation, NASA TN D-2872, 1965.

Baldwin, Jr. B. S., and H. J. Allen, A method for computing luminous efficiencies from meteor data, NASA TN D-4808, 1968.

Centolanzi, F. J. and D. R. Chapman, Vapor pressure of tektite glass and its bearing on tektite trajectories determined from aerodynamic analysis. J. Geophys. Res. 71, 1735-1749, 1966.

Kornblum, J. J., Micrometeoroid interaction with the atmosphere. To be published in J. Geophys. Res. 1968a.

Kornblum, J. J., On the concentration and collection of meteoric dust in the atmosphere. To be published in J. Geophys. Res., 1968b.

Lebedinec, V. N. and Suskova, Evaporation and deceleration of small meteoroids, in Physics and Dynamics of Meteors, Kresak and Millman, 193-204, I. A. U. conference, 1968.

Levin, B. I., Physical theory of meteors and meteoritic material in the solar system. Chapters I-III, translated from Russian by American Meteoritical Society, 1956.

Öpik, E. J., Physics of meteor flight in the atmosphere, Interscience, 1958.

Shoemaker, E. M., Interpretation of lunar craters, in Physics and Astronomy of the Moon, Z. Kopal, ed., Academic Press, 1962.

Table I

Meteoroid Vapor Pressure Law Parameters

$\text{Log } p = c_1 + c_2/T$ $\qquad$ p in N/m^2, T in °F

	c_1	c_2
Öpik stone[1]	9.6	-1.35×10^4
Öpik iron[1]	9.607	-1.612×10^4
Dushman iron[2]	12.53	-2.14×10^4
Tektite[3]	13.301	-2.5102×10^4
Norton County achondrite[4]	14.215	-2.67×10^4
Carbonaceous chondrite [synthetic][4] (volatile part)	11.613	-1.675×10^4
Carbonaceous chondrite [synthetic][4] (refractory part)	10.63	-1.674×10^4
Liebedinec Stone[5]	13.341	-2.505×10^4

1. Öpik [1958]
2. Levin [1956]
3. Centolonzi and Chapman [1966]
4. Ames Research Center, results quoted by Baldwin and Allen [1968]
5. Lebedinec and Suskoya [1968]

Table 2

Cases Examined

Entry Velocity V_∞, km/sec	Similarity Variable $\delta\ r_\infty \cos Z_\infty$, kg/m^2
70	250×10^{-3}
60	150×10^{-3}
50	100×10^{-3}
40	50×10^{-3}
30	25×10^{-3}
20	15×10^{-3}
15	10×10^{-3}
12	5×10^{-3}
	2.5×10^{-3}
	1.0×10^{-3}
	0.5×10^{-3}
	0.25×10^{-3}
	0.15×10^{-3}
	0.10×10^{-3}
	0.05×10^{-3}
	0.025×10^{-3}
	0.010×10^{-3}
	0.005×10^{-3}

Table 3

Effect of Density and Vapor Pressure Law

On Meteorite Ablation

Residual Radius for 30μ Radius Particle Entering Vertically at 30 km/sec

Assumed Density (g/cm^3)	$\delta r_\infty \cos Z_\infty$ (kg/m^2)	Vapor Pressure Law: Norton County Achondrite	Öpik Iron	Carbonaceous Chondrite	Öpik Stone
3.4	1.02×10^{-1}	0.6 μ	0.6 μ	0.11 μ	0.13 μ
3.0	$9. \times 10^{-2}$	0.9	0.75	0.16	0.18
2.5	7.5×10^{-2}	1.5	0.9	0.3	0.3
2.0	$6. \times 10^{-2}$	1.8	1.5	0.4	0.4
1.5	4.5×10^{-2}	3.0	2.4	0.54	0.6
1.0	$3. \times 10^{-2}$	5.7	4.2	0.9	1.1
0.85	2.55×10^{-2}	7.2	5.1	1.2	1.2
0.50	1.5×10^{-2}	18.0	12.0	3.0	3.0
0.25	7.5×10^{-3}	28.1	22.5	10.5	9.9
0.10	3×10^{-3}	30.0	30.0	25.5	24.3

Table 4

Shielding due to Meteoroid Vapors

Evaluated for meteoroid density x cos (zenith entry angle), $\delta \cos Z_\infty = 10^3 kg/m^3$

$\Psi = S/\delta \cos Z_\infty$

$\Psi = 1.0$ corresponds to complete shielding

I. Öpik stone vapor pressure law

Entry Radius (Microns)	70	60	50	40	30	20	15	12
			Entry velocity (km/sec)					
250	1.22	1.10	0.96	0.80	0.62	0.38	0.24	0.14
150	0.46	0.40	0.36	0.30	0.22	0.14	0.08	0.04
100	0.20	0.18	0.16	0.14	0.10	0.06	0.04	0.02
50	0.06	0.06	0.04	0.04	0.02	0.02	0.01	

II. Norton County Achondrite vapor pressure law

Entry Radius (Microns)	70	60	50	40	30	20	15	12
			Entry velocity (km/sec)					
250	1.32	1.18	1.02	0.86	0.66	0.40	0.20	0.08
150	0.50	0.44	0.40	0.34	0.26	0.14	0.06	0.01
100	0.24	0.20	0.18	0.16	0.12	0.06	0.02	
50	0.06	0.06	0.06	0.04	0.04	0.01		

Figure Captions

Figure 1. Energy dissipated by the particle as a function of surface temperature. The energy dissipated by radiation processes, E_R, and the energy dissipated by vaporization processes, E_v, per unit area per unit time for several proposed meteoroid vapor pressure laws are shown. Dashed lines represent the sum $(E_R + E_v)$ whenever it differs significantly from either E_R or E_v. (Figure reproduced from Kornblum, 1968 a).

Figure 2. Ablation effect on micrometeoroids for the Norton County Achondrite vapor pressure law. This case gives the least ablation. Final radius/entry radius vs. the similarity variable: meteoroid density x entry radius x cos (zenith entry angle), $\delta\ r_\infty \cos Z_\infty$.

Figure 3. Ablation effect on micrometeoroids for the Öpik Iron vapor pressure law. Final radius/entry radius vs. the similarity variable: meteoroid density x entry radius x cos (zenith entry angle), $\delta\ r_\infty \cos Z_\infty$.

Figure 4. Ablation effect on micrometeoroids for the synthetic carbonaceous chondrite vapor pressure law. Final radius/entry radius vs. the similarity variable: meteoroid density x entry radius x cos (zenith entry angle), $\delta\ r_\infty \cos Z_\infty$.

Figure 5. Ablation effect on micrometeoroids for the Öpik stone vapor pressure law. This case gives the most ablation. Final

radius/entry radius vs. the similarity variable: meteoroid density x entry radius x cos (zenith entry angle), $\delta\, r_\infty \cos Z_\infty$.

Figure 6. Residual particle radius vs. entry radius for the Norton County Achondrite vapor pressure law when meteoroid density x cos (zenith entry angle), $\delta \cos Z_\infty$, equals 3.4×10^3 kg/m^3.

Figure 7. Residual particle radius vs. entry radius for Öpik Iron vapor pressure law when meteoroid density x cos (zenith entry angle), $\delta \cos Z_\infty$, equals 3.4×10^3 kg/m^3.

Figure 8. Residual particle radius vs. entry radius for synthetic carbonaceous chondrite vapor pressure law when meteoroid density x cos (zenith entry angle), $\delta \cos Z_\infty$, equals 3.4×10^3 kg/m^3.

Figure 9. Residual particle radius vs. entry radius for Öpik stone vapor pressure law when meteoroid density x cos (zenith entry angle), $\delta \cos Z_\infty$, equals 3.4×10^3 kg/m^3.

Figure 10. Residual particle radius vs. entry radius for Norton County Achondrite vapor pressure law when meteoroid density x cos (zenith entry angle), $\delta \cos Z_\infty$, equals 0.85×10^3 kg/m^3.

Figure 11. Residual particle radius vs. entry radius for Öpik Iron vapor pressure law when meteoroid density x cos (zenith entry angle), $\delta \cos Z_\infty$, equals 0.85×10^3 kg/m^3.

Figure 12. Residual particle radius vs. entry radius for synthetic carbona-

ceous chondrite vapor pressure law when meteoroid density x cos (zenith entry angle), $\delta \cos Z_{\infty}$, equals 0.85×10^3 kg/m^3.

Figure 13. Residual particle radius vs. entry radius for Öpik stone vapor pressure law when meteoroid density x cos (zenith entry angle), $\delta \cos Z_{\infty}$, equals 0.85×10^3 kg/m^3.

Figure 14. Altitude where ablation ceases vs. the similarity variable: meteoroid density x entry radius x cos (zenith entry angle), $\delta\, r_{\infty} \cos Z_{\infty}$, for the Norton County Achondrite, Öpik Iron, synthetic carbonaceous chondrite, and Öpik stone meteoroid vapor pressure laws.

Figure 15. Maximum temperature reached by the meteoroids vs. the similarity variable: meteoroid density x entry radius x cos (zenith entry angle), $\delta\, r_{\infty} \cos Z_{\infty}$, for the Norton County Achondrite, Öpik Iron, synthetic carboneceous chondrite, and Öpik stone meteoroid vapor pressure laws.

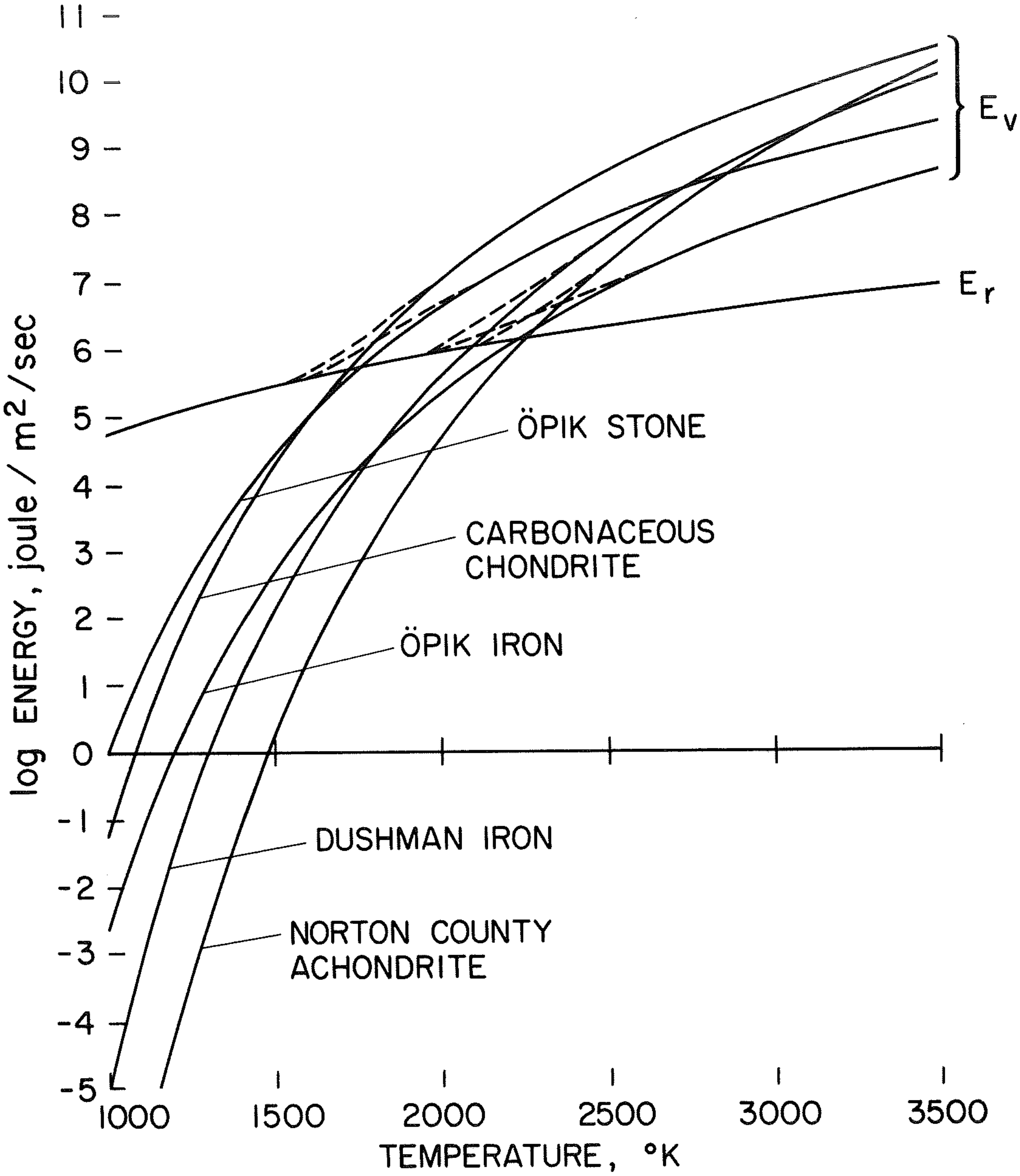
log ENERGY, joule / m²/sec
TEMPERATURE, °K
E_v
E_r
ÖPIK STONE
CARBONACEOUS CHONDRITE
ÖPIK IRON
DUSHMAN IRON
NORTON COUNTY ACHONDRITE

Figure 1.

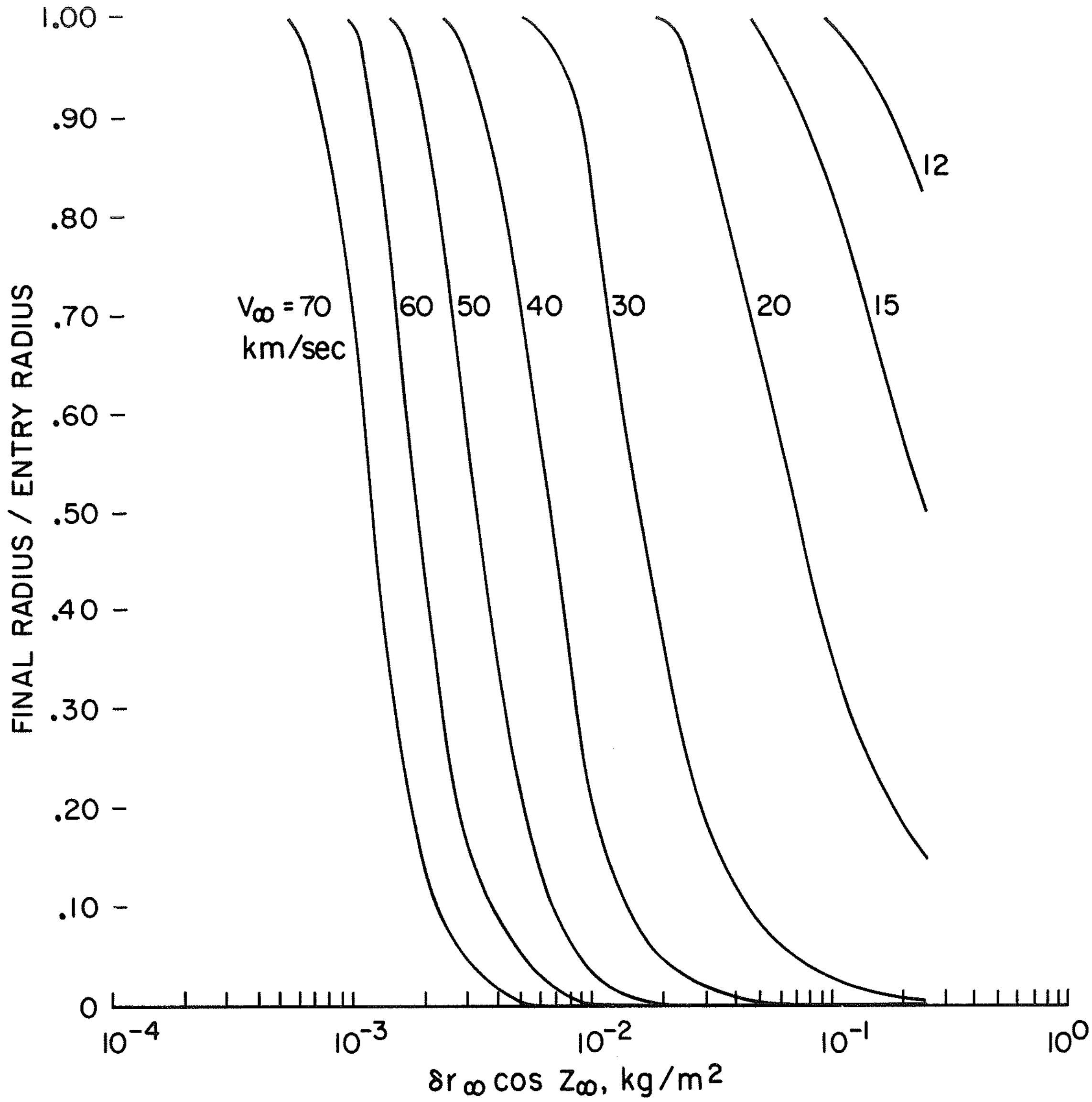

Figure 2.

NATIONAL AERONAUTICS AND SPACE ADMINISTRATION
AMES RESEARCH CENTER, MOFFETT FIELD, CALIFORNIA

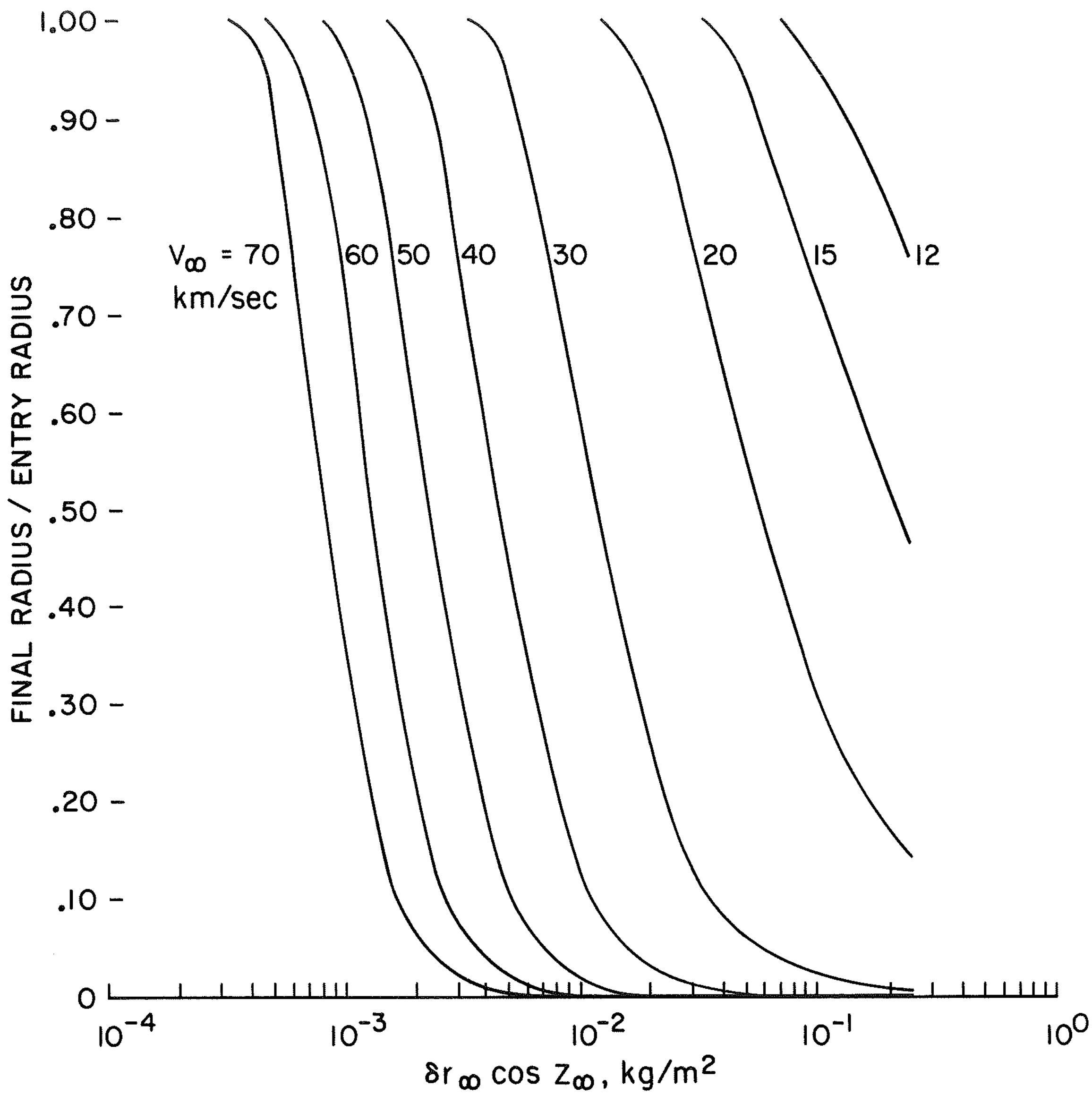
1.00
.90
.80
.70
.60
.50
.40
.30
.20
.10
0
FINAL RADIUS / ENTRY RADIUS
V_∞ = 70 km/sec
60
50
40
30
20
15
12
10^{-4}
10^{-3}
10^{-2}
10^{-1}
10^{0}
$\delta r_\infty \cos Z_\infty$, kg/m^2

Figure 3.

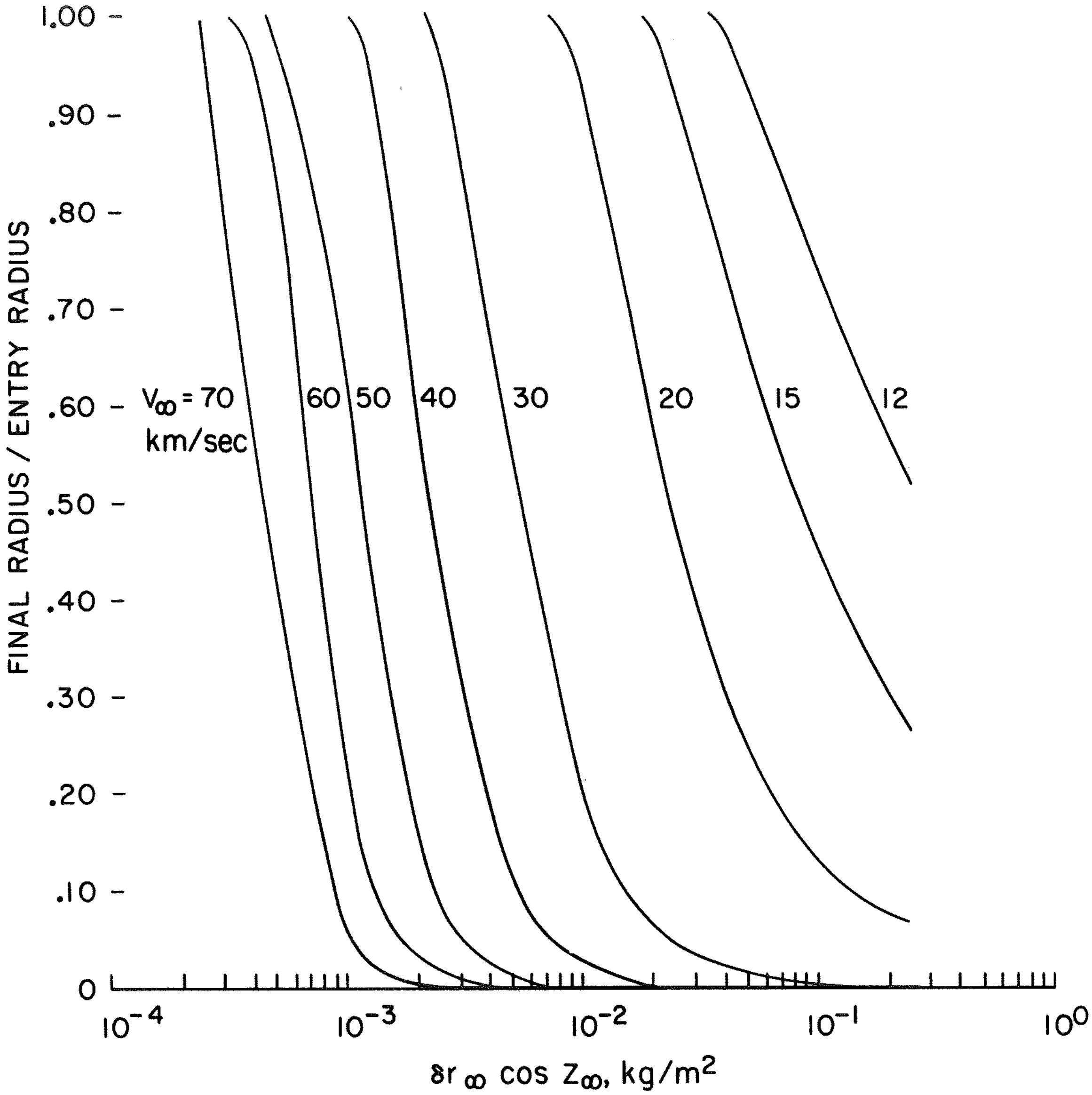

1.00
.90
.80
.70
.60
.50
.40
.30
.20
.10
0
FINAL RADIUS / ENTRY RADIUS
V_∞ = 70 km/sec
60
50
40
30
20
15
12
10^{-4}
10^{-3}
10^{-2}
10^{-1}
10^0
$\delta r_\infty \cos Z_\infty$, kg/m^2

Figure 4.

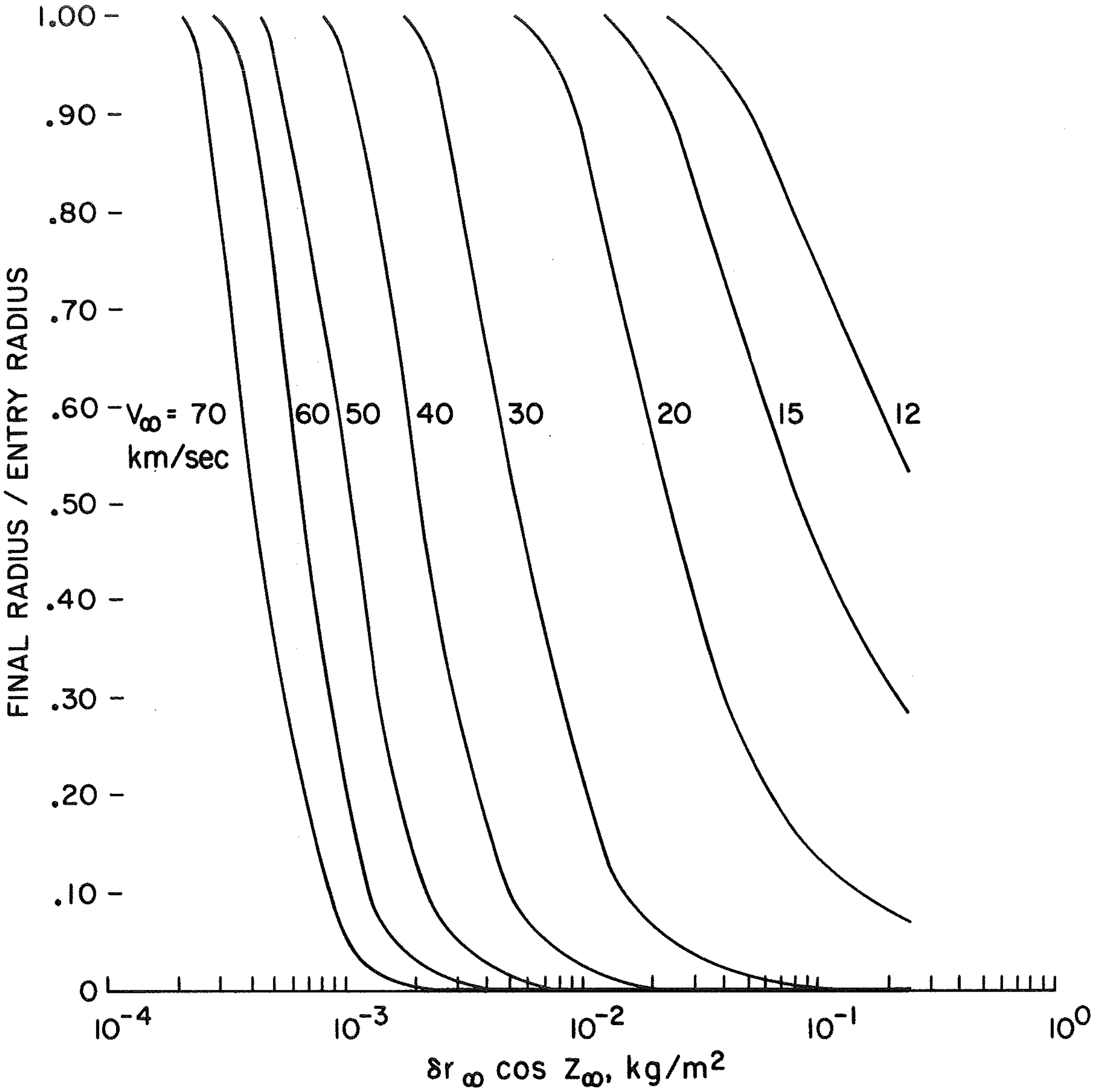
FINAL RADIUS / ENTRY RADIUS
1.00
.90
.80
.70
.60
.50
.40
.30
.20
.10
0
V_∞ = 70
km/sec
60
50
40
30
20
15
12
10^{-4}
10^{-3}
10^{-2}
10^{-1}
10^{0}
$\delta r_\infty \cos Z_\infty$, kg/m^2

Figure 5.

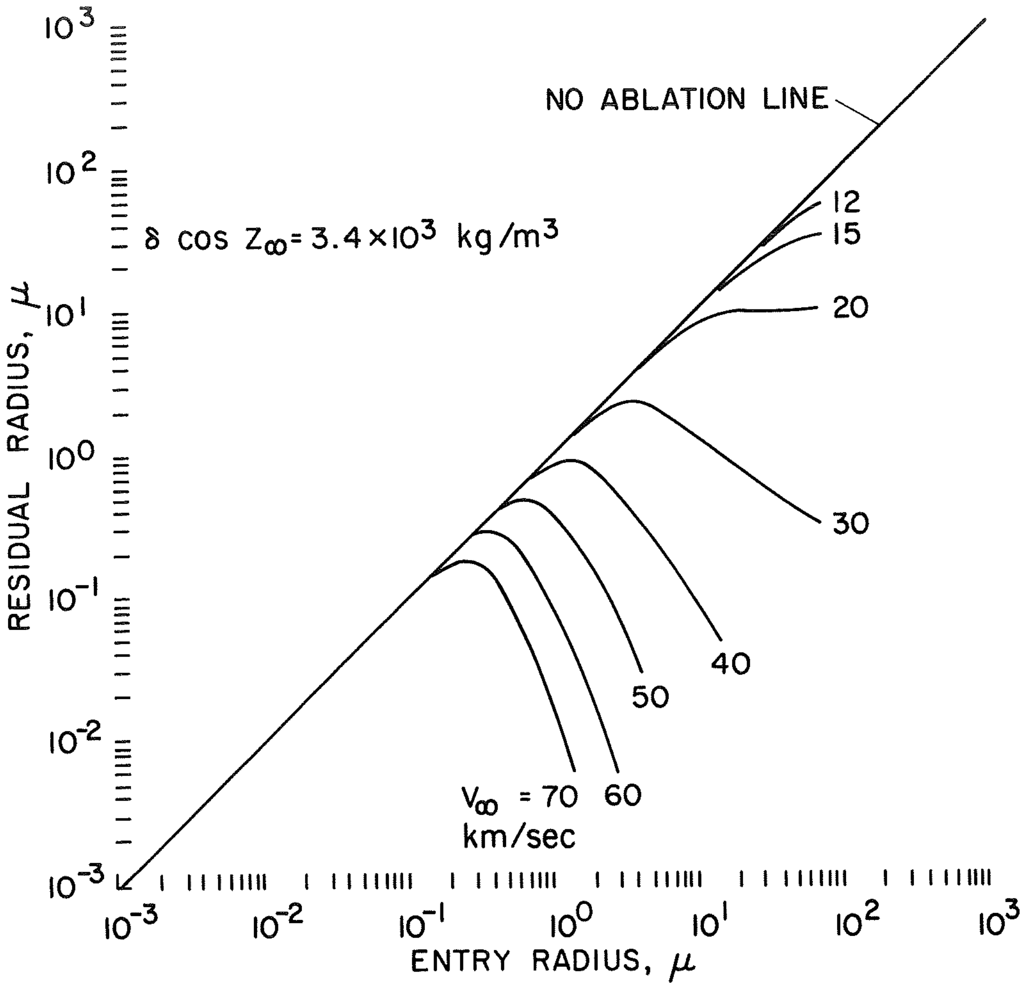

Figure 6.

NATIONAL AERONAUTICS AND SPACE ADMINISTRATION
AMES RESEARCH CENTER, MOFFETT FIELD, CALIFORNIA

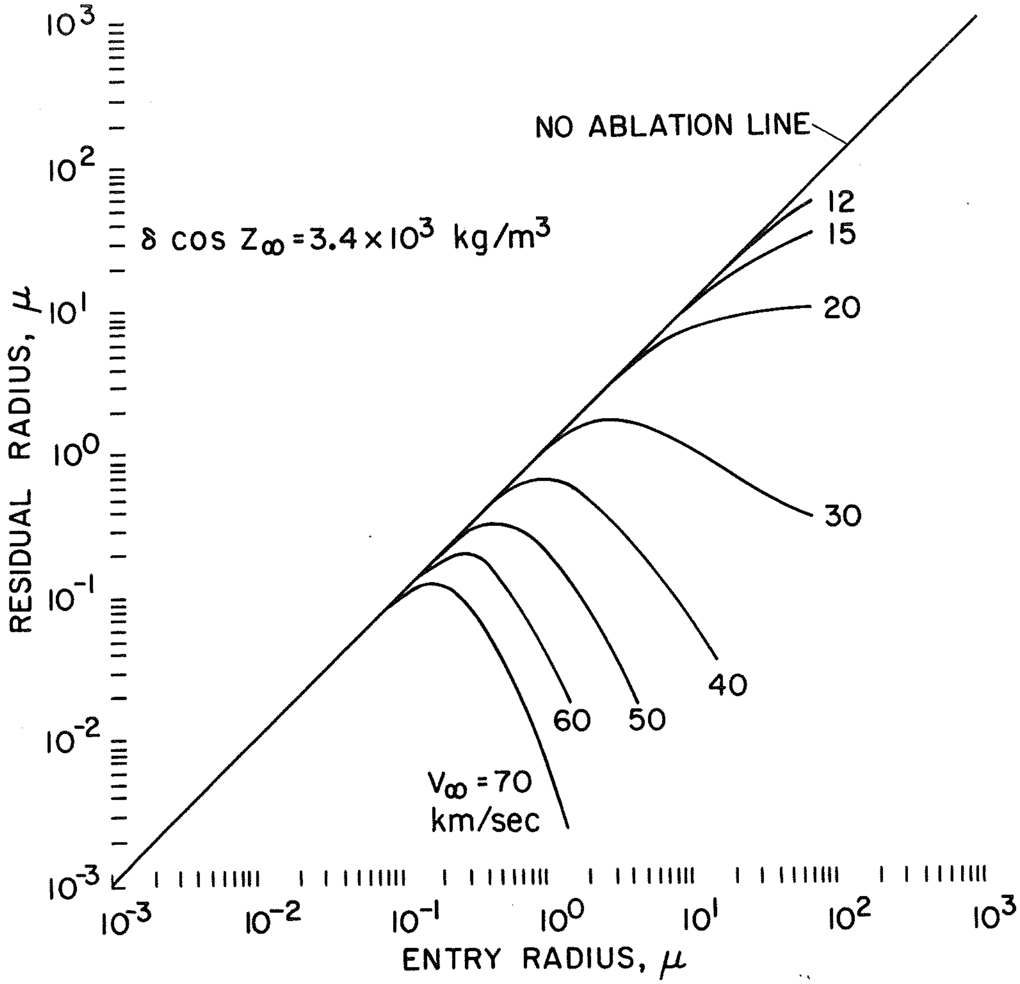

NO ABLATION LINE
$\delta \cos Z_\infty = 3.4 \times 10^3$ kg/m^3
12
15
20
30
40
50
60
$V_\infty = 70$
km/sec
RESIDUAL RADIUS, μ
ENTRY RADIUS, μ
10^{-3}
10^{-2}
10^{-1}
10^{0}
10^{1}
10^{2}
10^{3}

Figure 7.

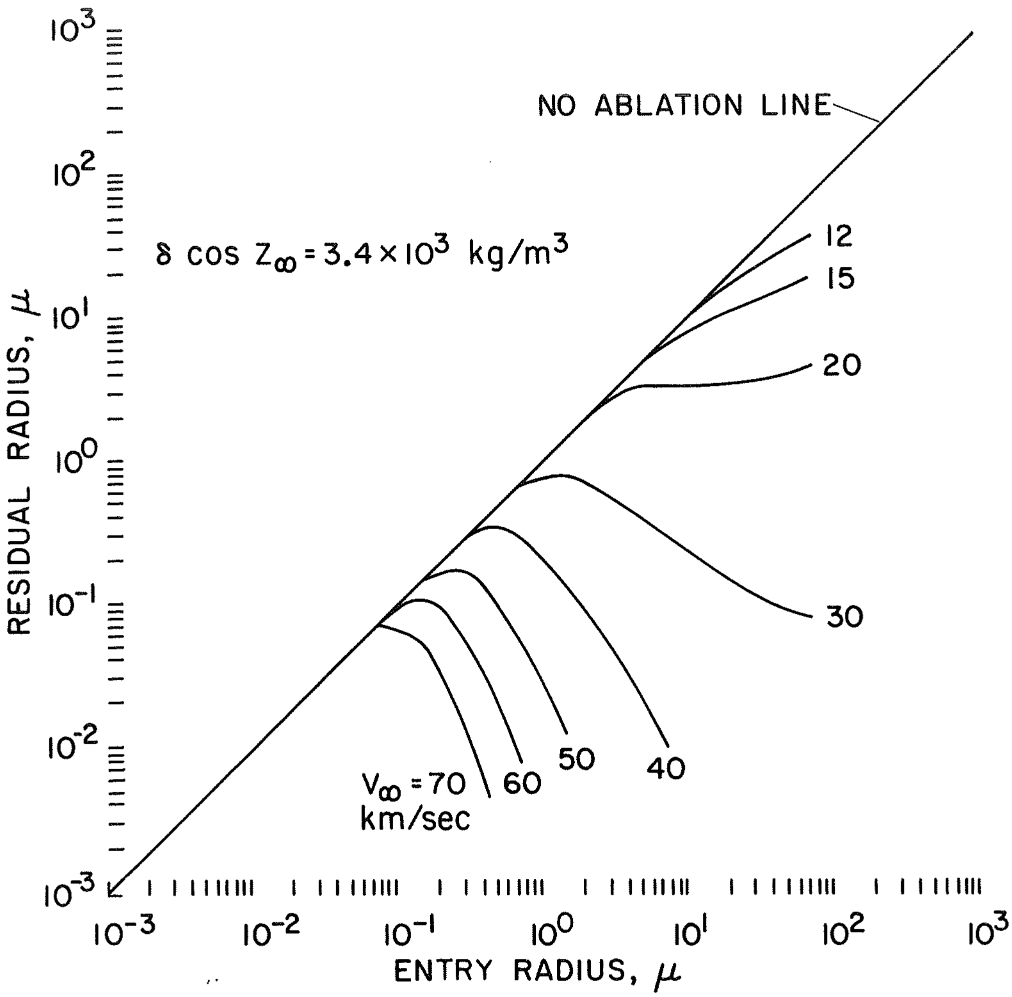
NO ABLATION LINE
δ cos Z∞ = 3.4×10³ kg/m³
RESIDUAL RADIUS, μ
ENTRY RADIUS, μ
12
15
20
30
40
50
60
V∞ = 70
km/sec
10⁻³
10⁻²
10⁻¹
10⁰
10¹
10²
10³

Figure 8.

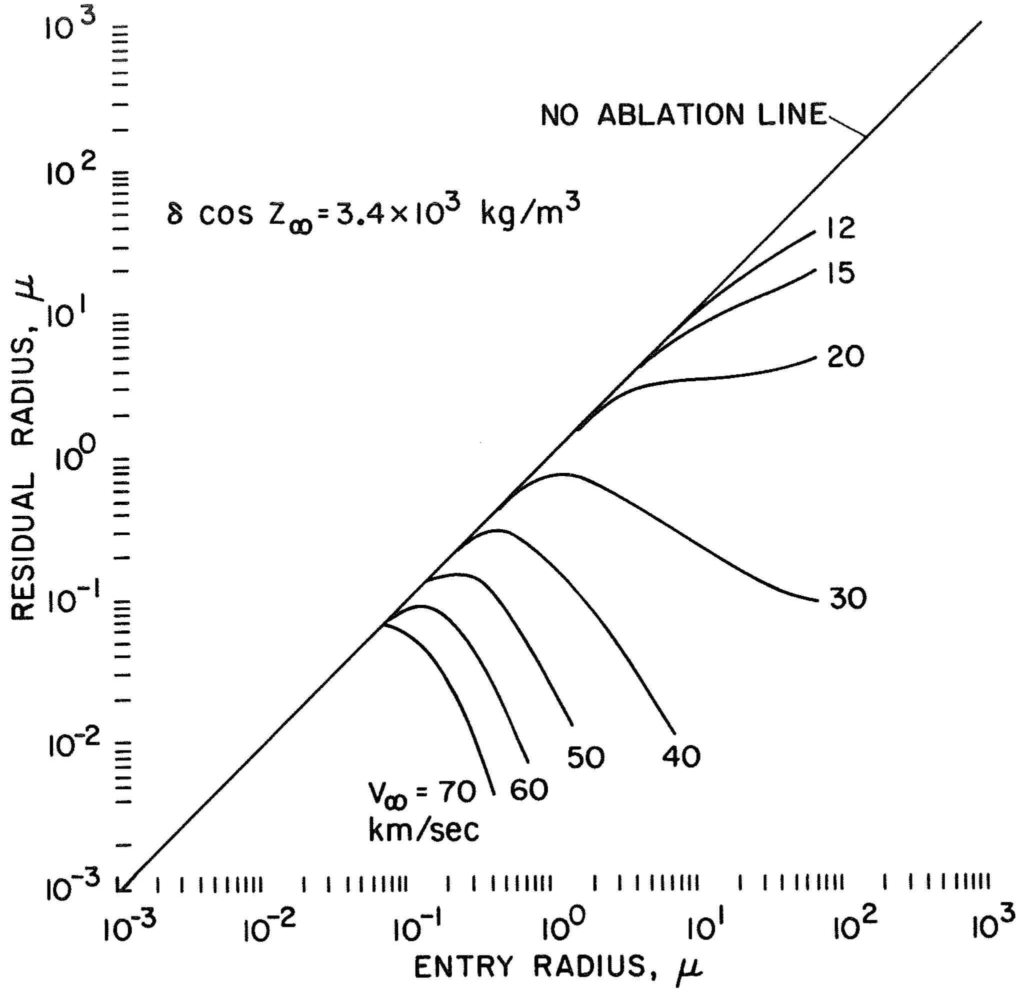

NO ABLATION LINE
$\delta \cos Z_\infty = 3.4 \times 10^3$ kg/m^3
12
15
20
30
50
40
V_∞ = 70
km/sec
60
RESIDUAL RADIUS, μ
ENTRY RADIUS, μ
10^{-3}
10^{-2}
10^{-1}
10^{0}
10^{1}
10^{2}
10^{3}

Figure 9.

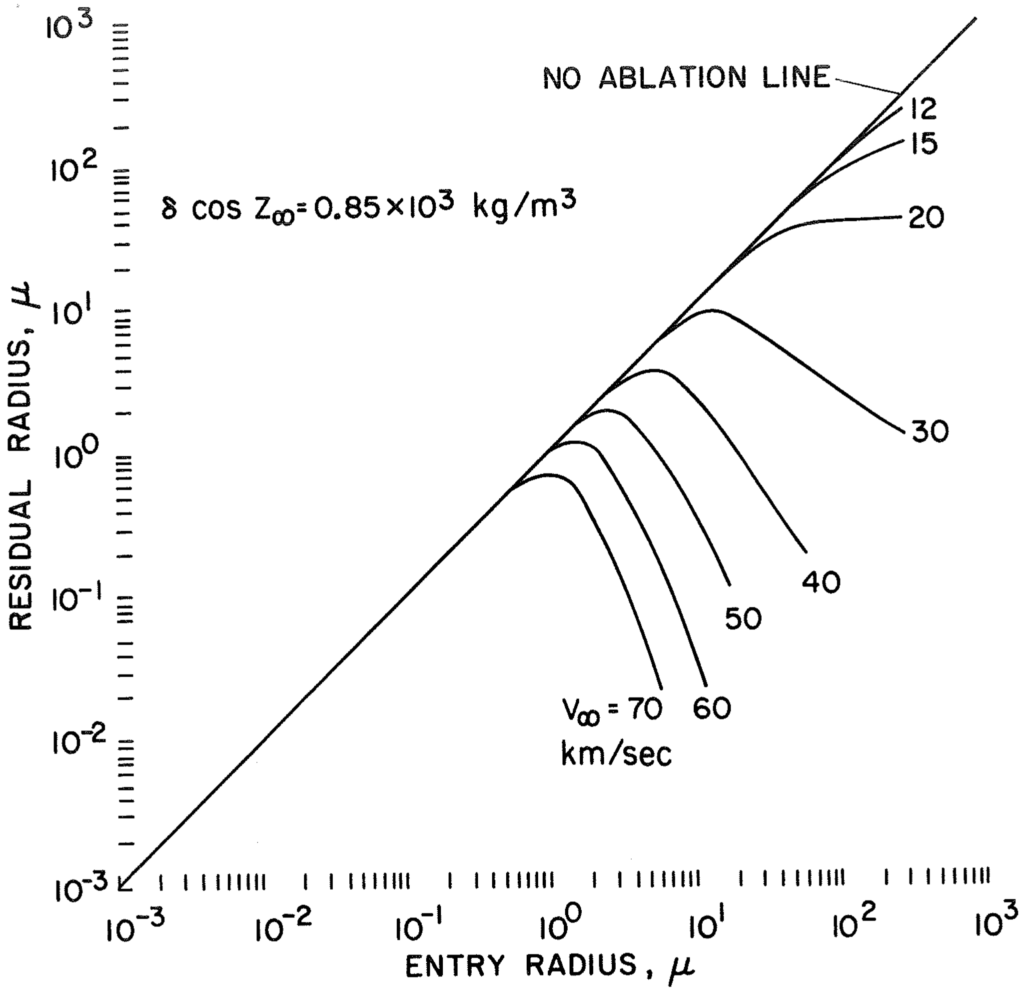

NO ABLATION LINE
12
15
20
30
40
50
V_∞ = 70 60
km/sec
δ cos Z_∞ = 0.85×10³ kg/m³
RESIDUAL RADIUS, μ
ENTRY RADIUS, μ
10⁻³
10⁻²
10⁻¹
10⁰
10¹
10²
10³

Figure 10.

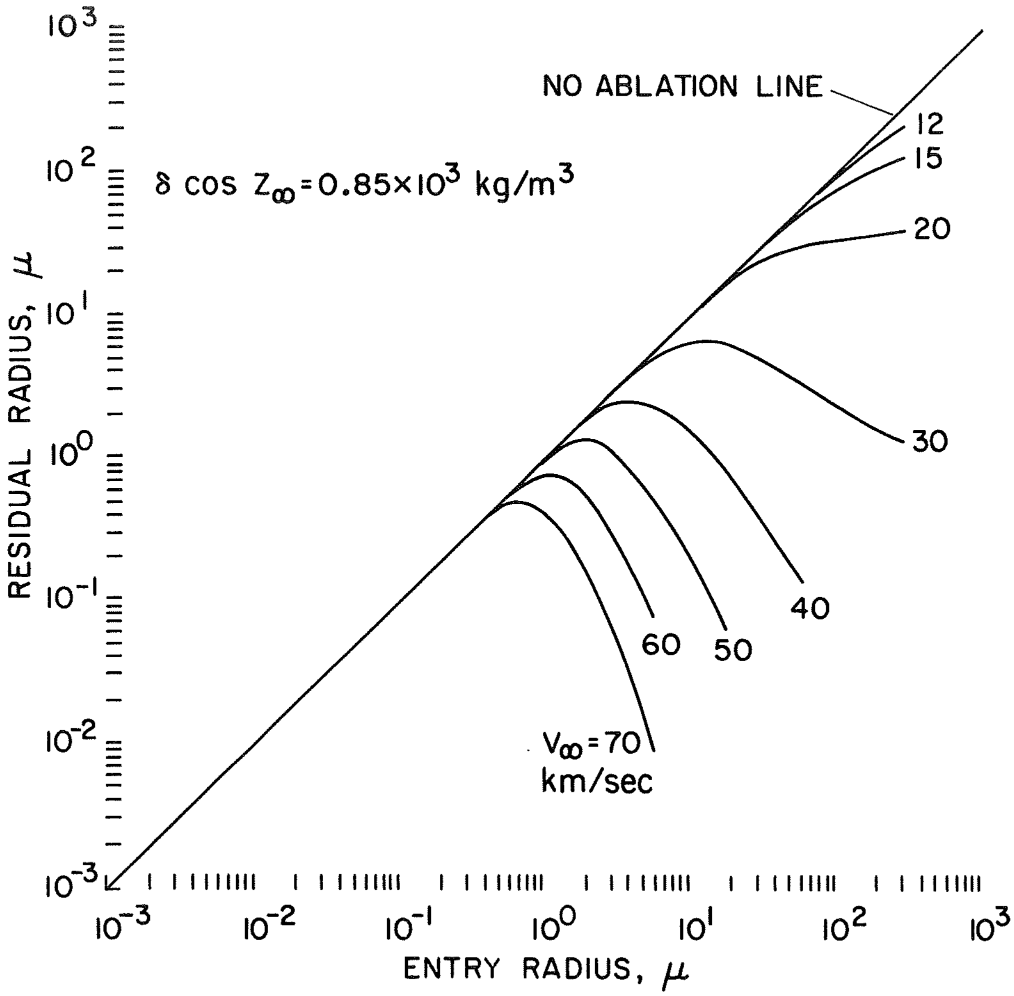
NO ABLATION LINE
12
15
20
30
40
50
60
V_∞=70 km/sec
$\delta \cos Z_\infty = 0.85 \times 10^3$ kg/m^3
RESIDUAL RADIUS, μ
ENTRY RADIUS, μ
10^{-3}
10^{-2}
10^{-1}
10^0
10^1
10^2
10^3

Figure 11.

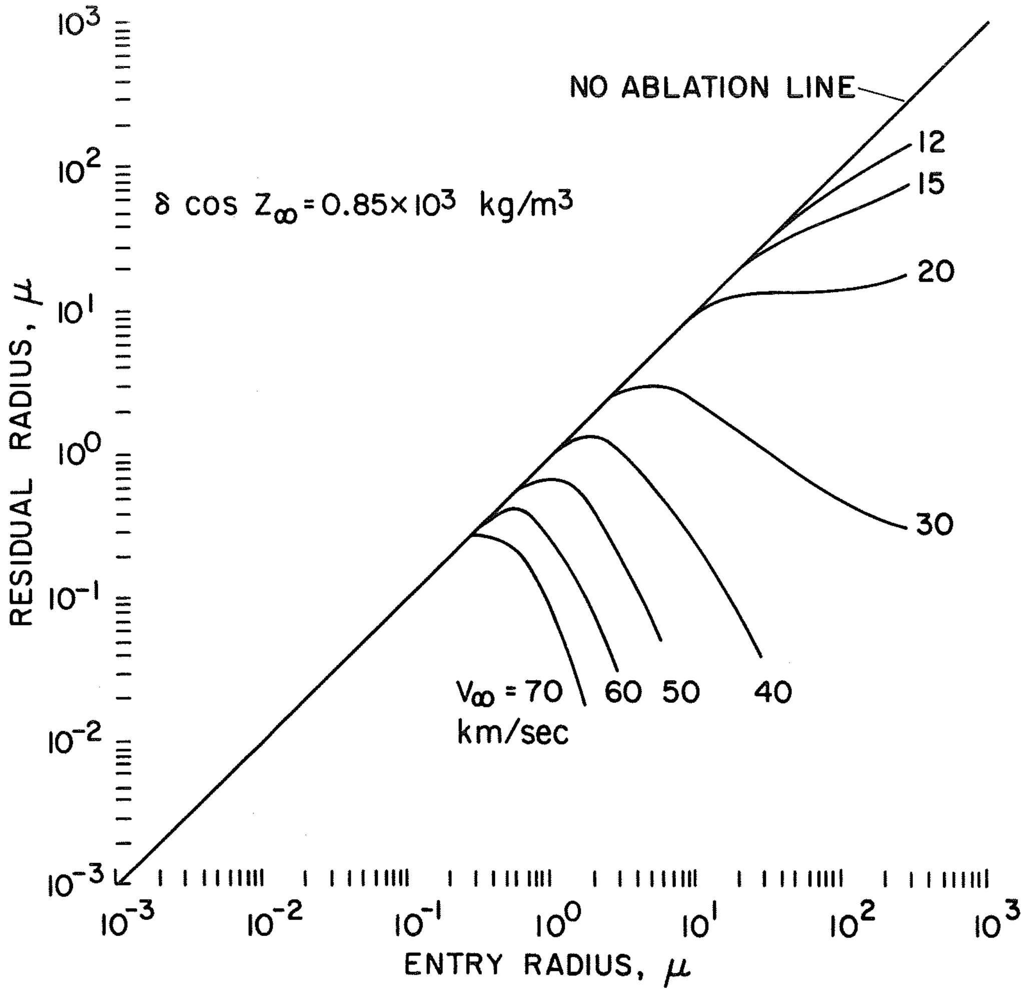

Figure 12.

NATIONAL AERONAUTICS AND SPACE ADMINISTRATION
AMES RESEARCH CENTER, MOFFETT FIELD, CALIFORNIA

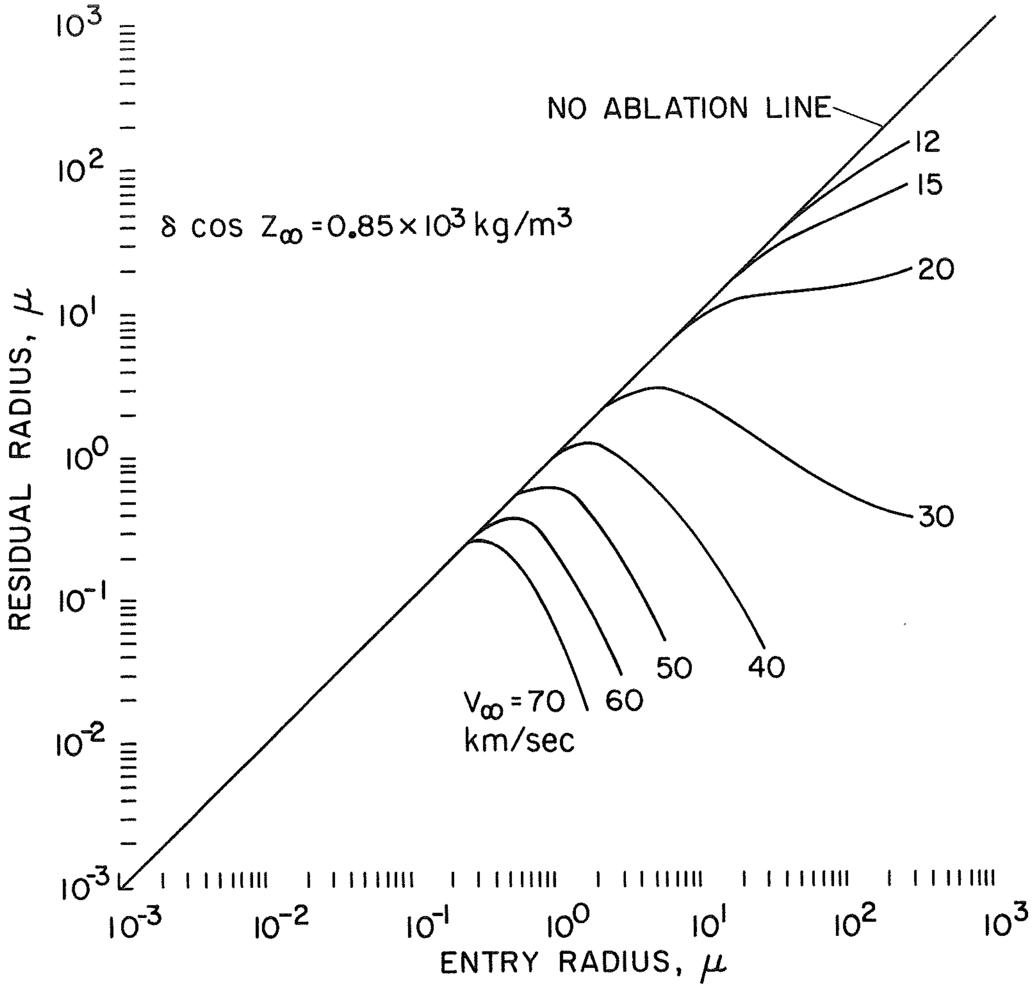
NO ABLATION LINE
12
15
20
30
40
50
60
$V_\infty = 70$ km/sec
$\delta \cos Z_\infty = 0.85 \times 10^3$ kg/m^3
RESIDUAL RADIUS, μ
ENTRY RADIUS, μ
10^{-3}
10^{-2}
10^{-1}
10^{0}
10^{1}
10^{2}
10^{3}

Figure 13.

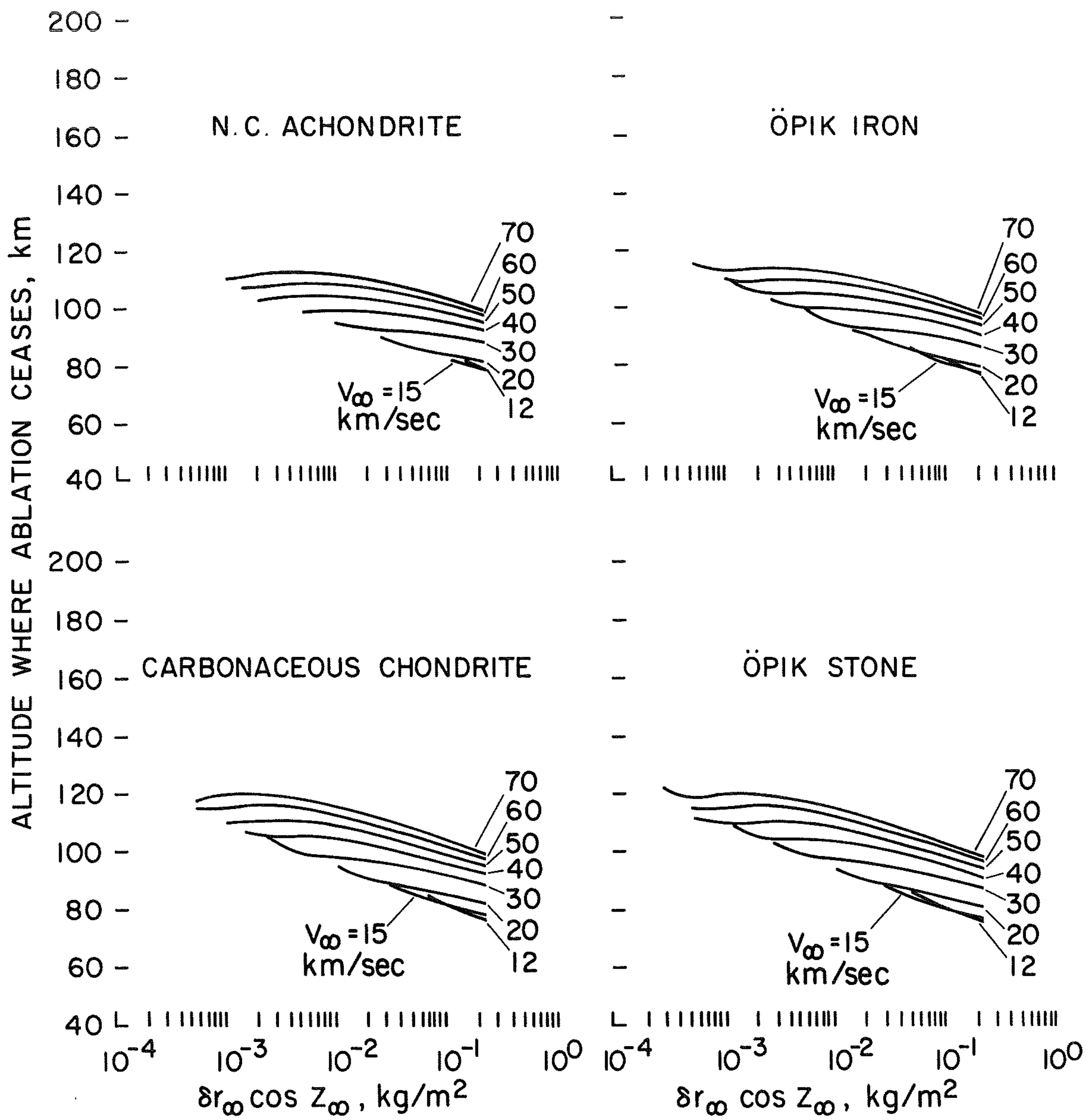

Figure 14.

NATIONAL AERONAUTICS AND SPACE ADMINISTRATION
AMES RESEARCH CENTER, MOFFETT FIELD, CALIFORNIA

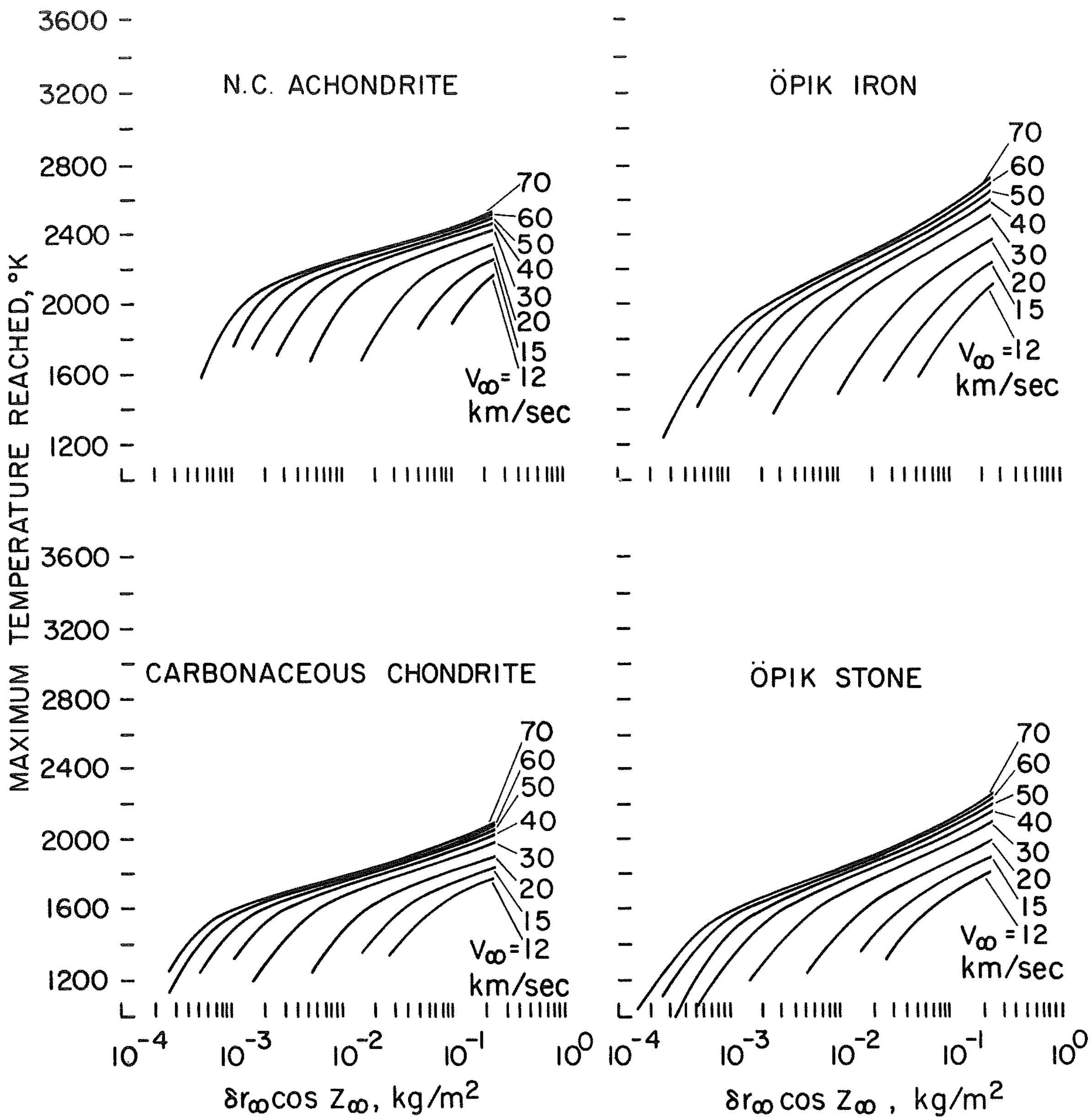
N.C. ACHONDRITE
ÖPIK IRON
CARBONACEOUS CHONDRITE
ÖPIK STONE
MAXIMUM TEMPERATURE REACHED, °K
3600
3200
2800
2400
2000
1600
1200
70
60
50
40
30
20
15
V∞ = 12
km/sec
10^-4
10^-3
10^-2
10^-1
10^0
δr∞ cos Z∞, kg/m²

Figure 15.